Optimal multicriteria approach to the iterative Fourier transform algorithm

Laurent Bigue, Pierre Ambs

Optimal multicriteria approach to the iterative Fourier transform algorithm

Laurent Bigué and Pierre Ambs

We propose a unified approach to the multicriteria design of diffractive optics. A multicriteria version of the direct binary search that allows the user to adjust the compromise between the diffraction efficiency and the signal-to-noise ratio already exists. This technique has proved to be extremely powerful but also very time consuming. We extend this multicriteria approach to the iterative Fourier transform algorithm, which helps to reduce the computation time dramatically, especially for multilevel domains. Simulations as well as experimental validations are provided.

OCIS codes: 090.1760, 090.1970.

1. Introduction

Since the inception of diffractive optical elements (DOEs) in the 1960s, many powerful methods have been proposed to compute them within the framework of the scalar diffraction theory. Nowadays, two kinds of techniques, both iterative, are mainly used: on the one hand, techniques derived from the direct binary search[1] (DBS), and, on the other hand, techniques derived from projection onto convex sets[2] (POCS) or the Gerchberg–Saxton algorithm.[3] Among the latter methods, the iterative Fourier transform algorithm (IFTA) technique proposed by Wyrowski and Bryngdahl[4] generally offers a good compromise between computation requirements and performance.

Legeard *et al.*[5] recently proposed an optimized multicriteria approach that allows the user to adjust a trade-off between the diffraction efficiency η and the amplitude error Err_a. This technique is based on a modified version of the DBS that easily helps in dealing with this trade-off adjustment. In this paper, we propose to extend this approach to the IFTA to drastically reduce the computing requirements that the DBS implies. We show that the IFTA can be transformed simply into a tunable, easily tractable, multicriteria technique because the adjustment of a single parameter is required. The DBS and the IFTA can then be considered together in a single multicriteria approach.

2. Optimal Trade-Off Design Basics

The concept of optimal trade-offs (OTs) was first presented to the optical community by Réfrégier.[6] Originally, it was applied to correlation filters; it was then extended by Legeard *et al.*[5] to DOEs. OT DOEs[5] are DOEs that, given $N-1$ criteria, optimize another criterion. The overall concept of OTs provides a practical framework for the study of DOEs because it allows any type of DOE to be included.

As is suggested in the literature, let us consider an element $\mathbf{h}$, which is not necessarily an OT element in the beginning, by taking into account the optical efficiency $\eta(\mathbf{h})$ and the accuracy of the reconstruction [characterized by the amplitude error $\mathrm{Err}_a(\mathbf{h})$] that are defined as

$$\eta(\mathbf{h}) = \frac{\sum_{k\in\Re} |\mathbf{g}_k|^2}{MN}, \tag{1}$$

$$\mathrm{Err}_a(\mathbf{h}) = \frac{\sum_{k\in\Re} (|\mathbf{f}_k| - \alpha|\mathbf{g}_k|)^2}{\sum_{k\in\Re} |\mathbf{f}_k|^2}, \tag{2}$$

$$\alpha = \frac{\sum_{k\in\Re} |\mathbf{f}_k||\mathbf{g}_k|}{\sum_{k\in\Re} |\mathbf{g}_k|^2}, \tag{3}$$

L. Bigué (L.Bigue@uha.fr) and P. Ambs (P.Ambs@uha.fr) are with the Groupe Fonctions Optiques et Traitement de l'Information (FOTI), Laboratoire Modeling Intelligence Process Systems (MIPS), Ecole Supérieure des Sciences Appliquées pour l'Ingénieur-Mulhouse (ESSAIM), Université de Haute Alsace, 12 rue des Frères Lumière, 68093 Mulhouse cedex, France.

Received 12 January 2001; revised manuscript received 5 June 2001.

0003-6935/01/325886-08$15.00/0

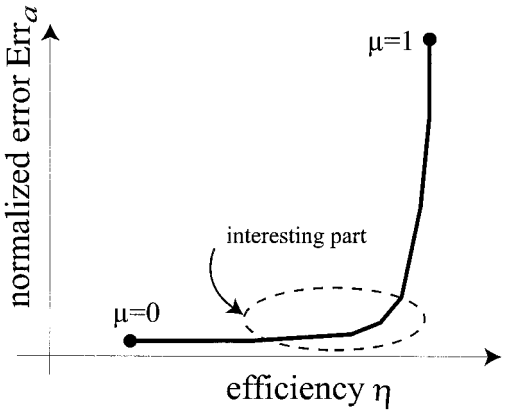

Fig. 1. Typical OCC for the criteria (η, Err_a) for the trade-off parameter μ as it varies from 0 to 1. The most interesting part is highlighted.

where **f** represents the desired pattern, **g** is the pattern reconstructed by the hologram **h**, $\Re$ is the region of interest (ROI), i.e., the desired part of the reconstruction but not the whole reconstruction plane, and *MN* is the number of pixels in the diffractive element. The criteria and Err_a are clearly antagonistic.

A DOE $\mathbf{h}_0$ is said to be an OT DOE for the two criteria η and Err_a if there is no other DOE **h**, such as

$$\eta(\mathbf{h}_0) \leq \eta(\mathbf{h}), \qquad \mathrm{Err}_a(\mathbf{h}_0) \geq \mathrm{Err}_a(\mathbf{h}). \tag{4}$$

It has been shown that such an element **h** minimizes the cost function

$$E_\mu(\mathbf{h}) = \mu \frac{1}{\eta(\mathbf{h})} + (1 - \mu)\mathrm{Err}_a(\mathbf{h}), \tag{5}$$

where μ is a parameter characterizing the trade-off.

The concept of a trade-off among several criteria provides an efficient way to compare the performances of DOEs and their implementations in various coding domains. The point is to draw the locus of points described by the different criteria when we explore all the possible implementations (with μ varying) in a given coding domain $\mathcal{D}$. This locus of points is usually convex (except in the case of a local minimum during convergence) and is called the optimal-characteristics curve (OCC). Figure 1 depicts a typical OCC shape when the considered criteria are the efficiency and the normalized error. For each OCC, the most interesting part of the curve depends on the constraints of the considered application, but it is often considered that the part close to the bottom right-hand corner is the most interesting: Great improvement in the diffraction efficiency can be obtained at the expense of a very slight degradation of error.

It should be noted that the OT general framework is not limited in its the number of criteria and can be extended to global or spatial criteria, such as reconstruction uniformity and noise reduction. In this paper, for the sake of clarity, we limit our study to the trade-off between the diffraction efficiency and the reconstruction accuracy, which are the major criteria in this context.

3. Diffractive Optical Element Design

A. Existing Techniques

Two among the most powerful of techniques for DOE computation were conceived in the 1980s: Wyrowski[7,8] and Wyrowski and Bryngdahl[4] proposed the IFTA, whereas Seldowitz *et al.*[1] proposed the DBS.

The IFTA, derived from the Gerchberg–Saxton algorithm[3] and closely related to POCS[2] and generalized POCS (which might not be convex[9]), is known to provide a good compromise between the computation requirements and the accuracy of the reconstruction and so proves to be very popular. We describe it more precisely in Subsection 3.B.

The DBS, a Monte Carlo technique, is known to be computer intensive but also extremely accurate, usually more so than the POCS-derived techniques,[5,10] especially when used with a simulated-annealing optimization. Legeard *et al.*[5] proposed using the IFTA as a preprocessing technique to the DBS, which combines the accuracy of the DBS with the reduced computer requirements of the IFTA. Because the DBS relies explicitly on criterion optimization, it has been extended to a multicriteria version[5] that consists of minimizing the cost function $E_\mu(\mathbf{h})$ described in Eq. (5).

B. Multicriteria Iterative Fourier Transform Algorithm

We are interested in developing a multicriteria version of the IFTA. Because the IFTA, described in Fig. 2 for the design of binary-amplitude holograms, does not rely explicitly on criterion optimization, it is not as straightforward as the DBS. In Wyrowski's studies[7,8] the goal was to provide an error-free reconstruction within the signal window, while maximizing the diffraction efficiency, possibly close to the theoretical maximum. Scale, amplitude, and phase degrees of freedom were used to do so. Such techniques led to the search for a unique solution. The multicriteria idea consists of loosening the constraint of producing an error-free reconstruction. Such an idea may sound strange, but it provides interesting insight: The point is to introduce a supplementary degree of freedom such that even the slightest loss of reconstruction accuracy can provide a high gain in the diffraction efficiency. In that sense, we cannot claim that the multicriteria IFTA is better than the IFTA; it just provides extra solutions. For the same requirements, it works in exactly the same way, but it enlarges the IFTA's range of applications when looser constraints than usual are applied.

Anyway, the first task is to find a parameter whose variations modify the convergence performance significantly in terms of criteria. As described by Fig. 2, the IFTA consists of performing successive iterations between the spatial and the spectral domains. The algorithm is divided into a given number of cycles of a given number of iterations. The spectrum con-

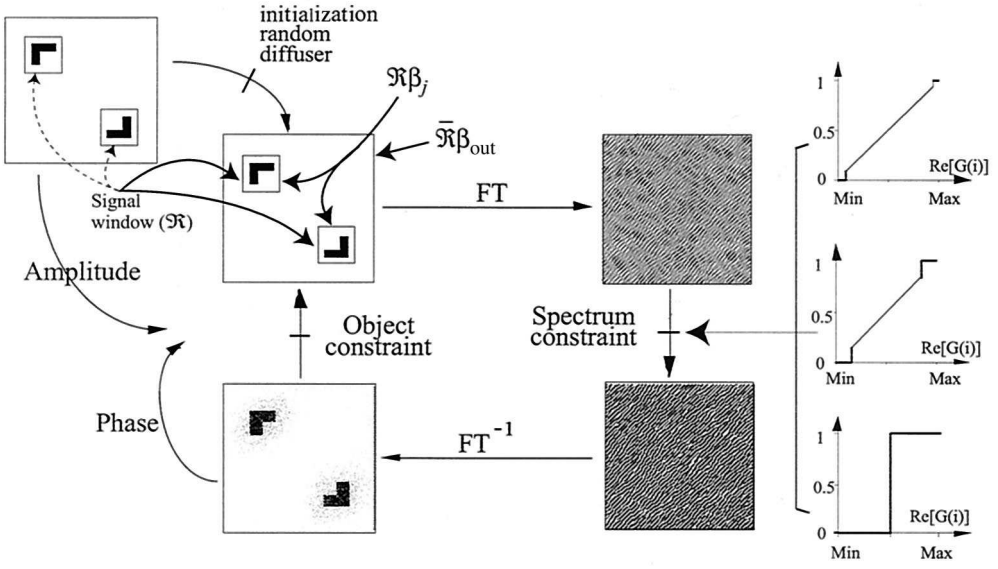

Fig. 2. Principle of the IFTA for the design of binary-amplitude holograms. β_{out} is applied in the object plane and in $\Re$ (i.e., outside the ROI $\Re$) and is less than 1; the scaling factor β_j applies to $\Re$ only. In the classical IFTA, β_j is fixed to 1, whereas it varies in the multicriteria IFTA, as explained in Section 3. FT, Fourier transformation.

straint, i.e., the choice of quantization bounds, is fixed over a cycle.

The possible parameters that we can tune are the number of cycles, the number of iterations per cycle, and the scaling factor β_j.[7] *A priori*, the number of iterations and the number of cycles do not play a significant role in the search for a compromise; a few simulations prove that they actually do not. On the other hand, β_j, which allows the noise to be rejected from the ROI and thus allows the error to be reduced, might play an important role in finding the compromise we are looking for. In previous studies[7] β_j was constrained to an optimized value, depending on the available degrees of freedom.

Actually, we want to use a parameter that makes sense within the OT framework, i.e., the trade-off parameter μ. The idea is to apply the scaling factor β_j (depending on μ) inside the ROI $\Re$. If we state that the value of $\mu = 0$ corresponds to the optimization of only Err_a and $\mu = 1$ to the optimization of only η, then μ and β_j should vary in the same direction.

Fetthauer *et al.*[11] had a similar idea, but they reported mainly nonantagonistic behavior between the two criteria the signal-to-noise ratio (SNR) and the diffraction efficiency, which led them to consider not a series of OTs but a unique compromise that seems optimal: Their version of the IFTA might be very different from ours because the IFTA would be seen as a framework, with many various derivatives and many parameters to tune, rather than as a definitive algorithm. Recently, Brenner[12] proposed an updated version of the idea of Fetthauer *et al.*[11] that consists of a relaxed projection operator in the Fourier plane that is known to provide stability during the convergence process. The relaxed projection parameter is optimized to vary over the cycles.

A few tries rapidly show that, if the scaling factor β_j is less than unity, the algorithm diverges, leading to a null solution (it probably corresponds in Ref. 11 to the lowest values of the scaling factor μ^f), and is of no interest to us. We finally choose

$$\beta_j = (MN)^{\mu}, \tag{6}$$

where MN represents the reconstruction space–bandwidth product. The power function in Eq. (6) provides stability because μ is positive only and the term MN has been empirically determined to ensure scaling: A few tests showed that no noticeable improvement in normalized criteria (larger than 10^{-3}) can be obtained with values of $\beta_j \gg MN$, as is detailed below in Section 4.

Figure 2 depicts the principle of the IFTA and the way that β_j is applied. We use a further parameter β_{out} in the uninteresting part of the image (the part outside $\Re$): We multiply this region, which is supposed to contain the noise rejected from the ROI, by β_{out}. The choice of an accurate value for β_{out} is discussed in Section 4 more precisely. Nevertheless, β_{out} will always be chosen to be less than one, which implies a reduction in the relative importance of the noise (the part of the image outside the ROI) in comparison with the ROI. We use, at the same time, β_{out} outside the ROI and β_j inside the ROI. Therefore the object-constraint operator can be expressed as

$$\mathbf{h}_k = \begin{cases} \mathbf{h}_k\beta_j & \text{if } k \in \Re \\ \mathbf{h}_k\beta_{out} & \text{else} \end{cases}. \tag{7}$$

Simultaneously using β_j and β_{out} as described above is not exactly equivalent to using the simpler modified operator

$$\mathbf{h}_k = \begin{cases} \mathbf{h}_k & \text{if } k \in \Re \\ \mathbf{h}_k \beta_{out}{}' = \mathbf{h}_k \dfrac{\beta_{out}}{\beta_j} & \text{else} \end{cases} \quad (8)$$

because of the nonlinearity of the quantization operator, the modified operator described in Eq. (8). However, producing a distribution similar to the one produced by the nonmodified operator of Eq. (7) (a scaled version, actually) modifies the overall energy of the reconstruction plane. As is explained in Section 4, a few tries showed that the use of two independent parameters, β_j and β_{out}, instead of one, $\beta_{out}{}'$, provided faster convergence of the whole algorithm. The use of the operator described in Eq. (7) is thus preferred.

4. Simulations

The diffractive elements presented in this paper are computed within the scalar diffraction theory framework, and they require a thin convergent lens to be reconstructed: They are Fourier diffractive elements.

Because our reconstruction algorithm basically consists of applying a Fourier transform to the distribution that describes our diffractive element, these elements may exhibit binary values (see Sections 4 and 5), multilevel values (see Section 4), or continuous values (not addressed in either simulations or experiments in this paper because, at present, no device available allows the reproduction of continuous gray-level values). No change in the reconstruction algorithm is required for this purpose.

All the simulations presented in this section concern 128×128 pixel DOEs that reconstruct various 32×32 pixel test images. According to research by Legeard,[13] the choice of a value for β_{out} depends on the constraints of the application. In this case, a binary Fourier diffractive element, the best choice is $\beta_{out} = 0.85$. Another choice, unless one chooses β_{out} greater than unity, will not make the algorithm diverge; it will only make it converge more slowly.

We first verified the concept of varying μ to tune the compromise between the optical efficiency and the error. As expected, if μ were chosen to be greater than one, the algorithm diverged rapidly. The value of the error obtained for $\mu = 0$ is the lowest attainable with the IFTA. For values of μ between 0 and 1 the efficiency increases at the expense of an increasing error. For negative values of μ the behavior obtained is similar to that reported by Fetthauer *et al.*[11] We do not report it in what follows because it is not an OT behavior. The evolution of the diffraction efficiency η versus the scaling factor β_j is illustrated in Fig. 3, which clearly shows the links between both parameters.

Figure 4 depicts the loci of points (η, error) that were obtained for various techniques and binary DOEs, and Table 1 reports the corresponding computation times for 128×128 pixels DOEs, depending on whether they are binary-amplitude or four-phase-level elements. Because the locus of the points (η, error) is now a full curve instead of a single point (as for the classical IFTA), Fig. 4 demonstrates that we have indeed obtained OT behavior. Moreover, it clearly shows that, when an iterative equalizer is

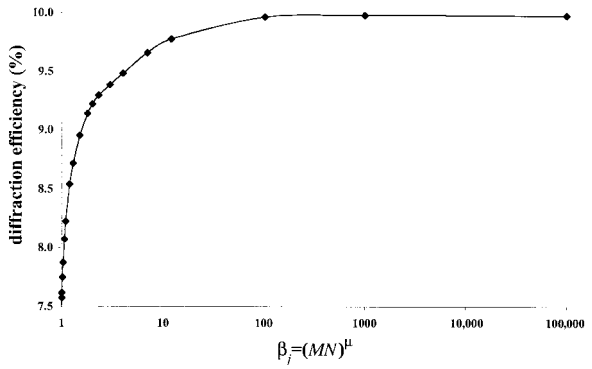

Fig. 3. Diffraction efficiency η plotted versus the scaling factor β_j for the case of a binary-amplitude coding domain.

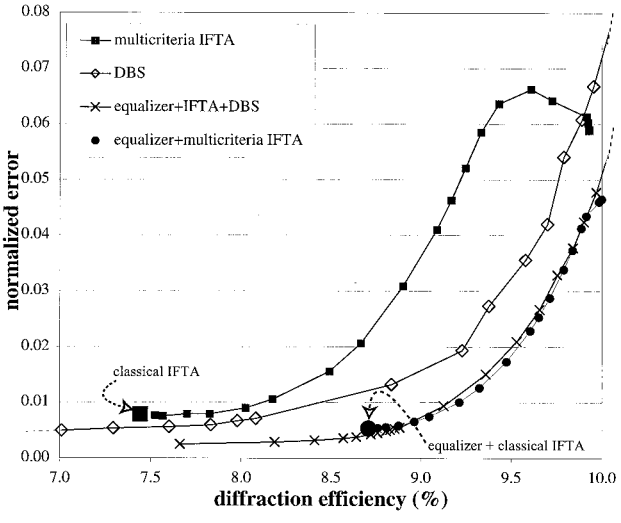

Fig. 4. Loci of points (η, error) for the variation of μ from 0 to 1 for various techniques and for binary-amplitude DOEs. For both multicriteria IFTA curves, i.e., with and without an equalizer, the points corresponding to the nonmulticriteria case are highlighted with a larger symbol.

Table 1. Typical Computation Times for 128×128 Pixel DOEs on a DEC Model AlphaStation 500 at 500 MHz by Use of Various Techniques

Design Technique	Type of DOE: Binary Amplitude (s)	Type of DOE: Four-Phase Level (s)
Equalizer plus IFTA plus DBS	160–630	500–1300
DBS	150–570	430–2000
Multicriteria IFTA	25	25
Equalizer plus multicriteria IFTA	75	75

used, the performance obtained with the IFTA is close to that provided by the DBS or even better, whereas the computation time is considerably reduced. Except for extreme cases in which a low error or a high efficiency is required, this outcome makes the IFTA the best possible candidate for DOE computation. As was suggested by Legeard *et al.*,[5] the equalizer used in this paper corresponds to an IFTA diffuser[14] with a modified spectrum constraint consisting of variable clipping. Hybrid input–output iterations[15] were also introduced for better and faster convergence. They consist of a Gerchberg–Saxton algorithm with relaxed projection in the reconstruction plane as given by

$$\mathbf{g}_{i+1}(k) = \begin{cases} (1-\gamma)\mathbf{g}_i(k) + \gamma\mathbf{f}_i(k) & k \in \Re \\ \mathbf{g}_i(k) & \text{else} \end{cases}, \tag{9}$$

where γ is the relaxation parameter, k is a pixel location, and i describes the iteration rank. Computation times reported for the four-phase-level elements show the huge increase in interest in the multicriteria IFTA over the multicriteria DBS: In the case of the IFTA, these computation times are almost completely independent of the number of levels N_1, whereas they grow similarly to N_1 with the DBS.

Another step in the OT design would have been to evaluate the criteria for a given parameter, to accept or reject the iterations according to the corresponding variations, and then to resume the algorithm with a modified parameter. We tested that algorithm and found that it did not improve the results significantly because the IFTA naturally and regularly converges to the desired minimum, so we came back to the original multicriteria IFTA described above.

5. Experimental Validation

We tested DOEs that were computed with the multicriteria IFTA on a twisted nematic liquid-crystal display (CRL, Model SVGA1). Although such devices show gray-level modulation capability,[16] we wanted to demonstrate that our technique works in the most stringent case, i.e., the binary case. We computed and tiled 256×256 elements that reconstructed the same gray level in a 153×60 pattern to the spatial light modulator (SLM) space–bandwidth product, 800×600, to reduce speckle. The Model SVGA1 SLM shows a 33-μm pixel pitch with a 0.57 fill factor and is operated at 60 Hz with 632.8-nm He–Ne radiation.

Figure 5 combines several views of the reconstruction plane for various values of μ, showing slightly degraded reconstructions as μ increases. However, these impressions are not sufficient to prove the OT behavior of our technique, and we performed an objective evaluation of its performance through precise measurements.

The summed point-to-point error Err_a was not evaluated because it is known to yield poor experimental values that are far from the real quality of the reconstructions. Incidentally, the question of evaluating the experimental reconstructions of diffractive elements has not yet been solved in a convincing manner. For removing speckle the elements are usually replicated, which leads to a sampled reconstruction plane. If we want to retrieve Err_a figures from this reconstruction plane, we need a camera, and the reconstruction sampling period must be an exact multiple of the camera sampling period to compute the sum of local differences expressed in Eq. (2). Thus the comparison of simulated and experimental figures does not prove to be straightforward, and this difficulty is probably why this complicated technique has never been reported to our knowledge.

Instead, we considered the noise-reduction ratio (NRR), as suggested by Moreno *et al.*,[17] which is expressed as

$$\mathrm{NRR} = \frac{E_{W(n,o)}}{E_{W(s,i)}}, \tag{10}$$

where $W(n, o)$ depicts a window containing noise that is outside the reconstruction window and $W(s, i)$ depicts the reconstruction window, i.e., the $\Re$. $E_{W(\ldots,\ldots)}$ is the energy evaluated within these windows. The NRR criterion should be used carefully. The less noise (and energy) outside the reconstruction window, the more energy within the reconstruction window. Then the diffraction efficiency increases when $E_{W(n,o)}$ decreases, but nothing ensures that this additional energy will not degrade the desired reconstruction.

We next evaluated a criterion that we named the simplified SNR (SSNR). This criterion corresponds to an evaluation of the error, summed over a window $W(n, i)$ that is inside the reconstruction window $W(s, i)$. To easily evaluate the error within $W(n, i)$, we chose $W(n, i)$ as a zone where the reconstructed signal should be zero. Then the SSNR is expressed as

$$\mathrm{SSNR} = \frac{E_{W(s,i)}}{E_{W(n,i)}}. \tag{11}$$

All the windows used in our experimental measurements are shown Fig. 6. We measured $E_{W(s,i)}$, $E_{W(n,i)}$, and $E_{W(n,o)}$ for various values of μ. Figure 7 reports the loci of points (η, 1/NRR) and (η, 1/SSNR) for the experimental data, and Fig. 8 shows the loci of points (η, Err_a) for the simulated data. In both cases, the diffraction efficiency is not scaled as Eq. (1) suggests, but, because it can be seen as an energy ratio and provided that the incident light does not vary, it has been replaced with the experimental measurement of the gray-level mean value of the energy in $\Re$. Both Figs. 7 and 8 clearly show OT behavior. We first note that, as anticipated, the NRR sometimes fails to evaluate the accuracy of the reconstruction correctly because it considers all the energy in the reconstruction window in the same manner, regardless of whether it is noise. Instead, Fig. 7 shows the antagonistic behavior of the SSNR and the efficiency. It clearly appears that, when μ increases, we obtain a significant improvement in efficiency at the expense of a slight

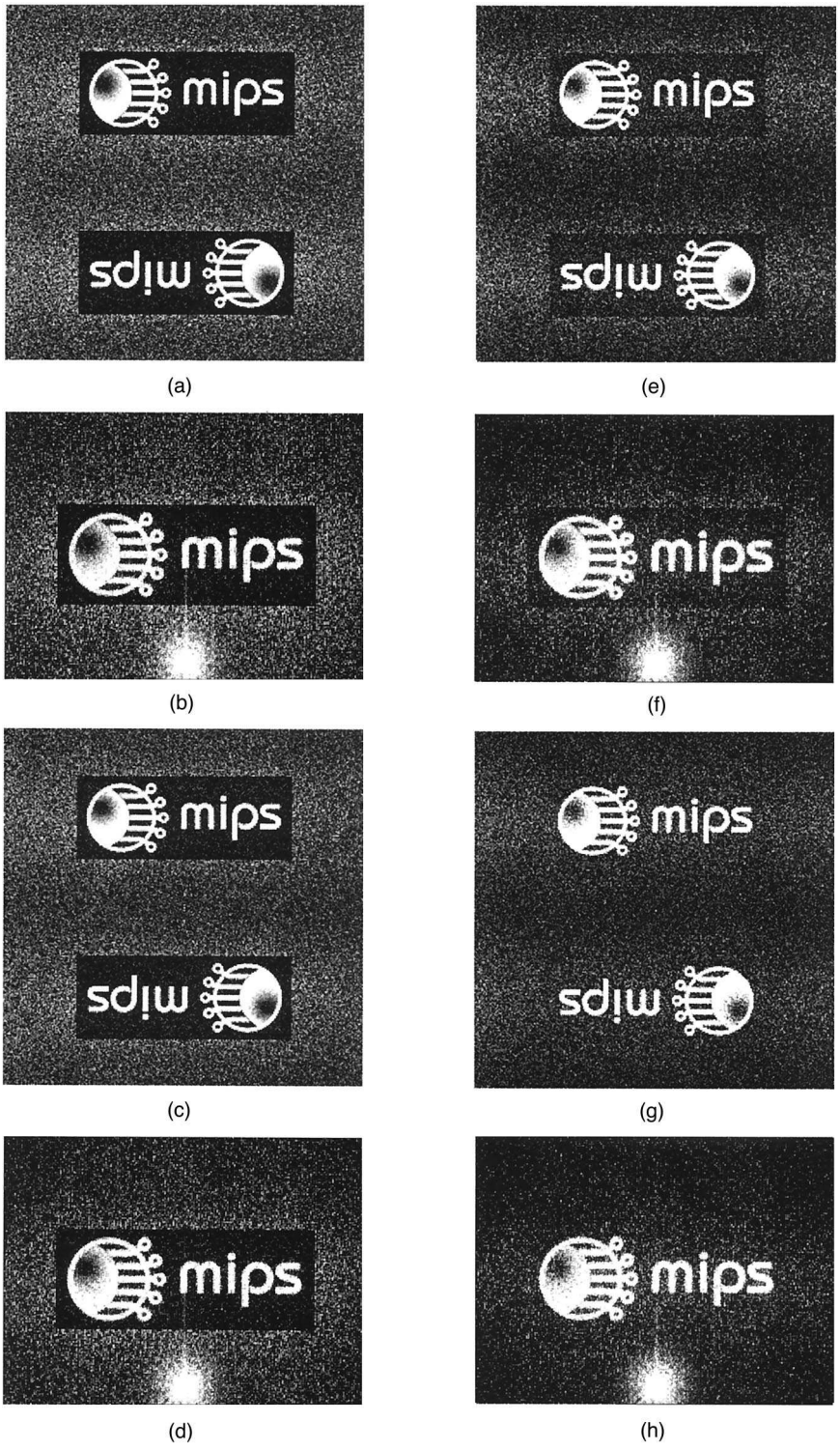

Fig. 5. Various reconstructions produced by the Model SVGA1 SLM operated in the binary mode. Simulations for different values of μ and their corresponding optical reconstructions are shown: (a) $\mu = 0$ and (b) its reconstruction; (c) $\mu = 0.01$ and (d) its reconstruction; (e) $\mu = 0.05$ and (f) its reconstruction; (g) $\mu = 0.999$ and (h) its reconstruction. When μ increases a degradation in image accuracy as well as an increase in the diffraction efficiency can be noted.

degradation in the SSNR, which is often hardly noticeable in the optical reconstructions: This is typical OT behavior. Further simulations and experiments show that this behavior is expressed more strongly (the OCC looks more like the typical shape shown in Fig. 1) when an iterative IFTA-like diffuser is used; but in that case, as in Fig. 4 with our test images, the range of variation in the efficiency is smaller.

Table 2 compares the simulated and the experimental implementations of the multicriteria IFTA.

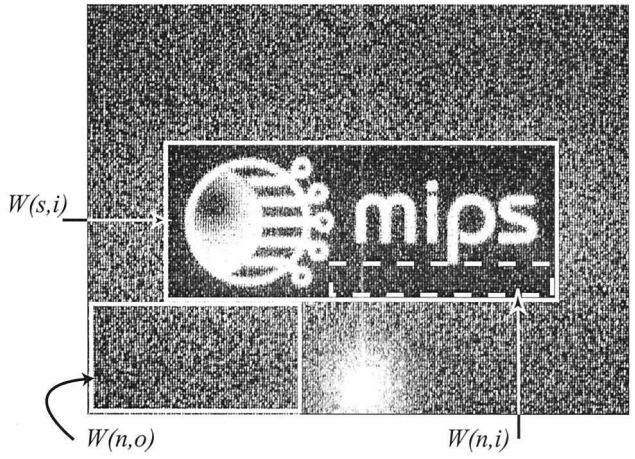

Fig. 6. All three windows used for our criteria evaluation: $W(s, i)$ is the signal window (ROI); $W(n, i)$ is used for the SSNR and is a noise window inside the signal window; $W(n, o)$ is used for the NRR and is a noise window outside the signal window.

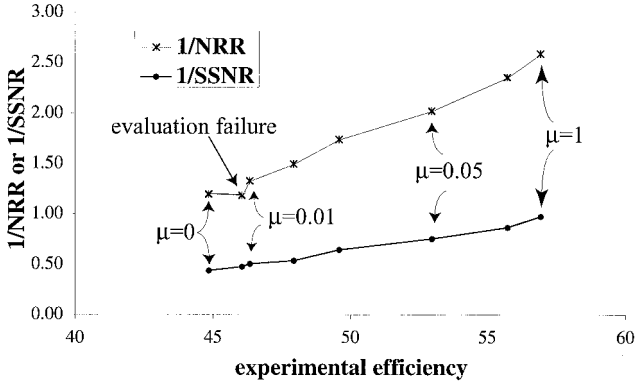

Fig. 7. Loci of points (η, 1/NRR) and (η, 1/SSNR) for the variation of μ from 0 to 1, corresponding to the experimental reconstructions shown in Fig. 5. The experimental efficiency η is defined as the mean energy expressed in terms of the gray-level value in the ROI $\Re$. As is highlighted, using the NRR may result in the incorrect evaluation of the reconstruction accuracy.

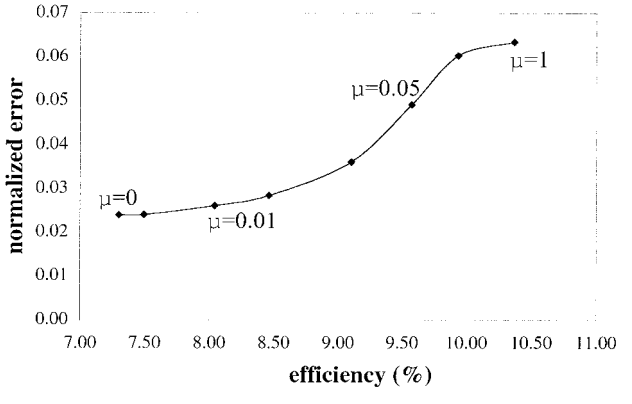

Fig. 8. Loci of points (η, Err_a) for the various values of μ that correspond to the simulated reconstructions shown in Fig. 5.

Table 2. Comparison of Simulated and Experimental Data

Data Type	Efficiency-Range Ratio[a]	Error-Range Ratio[b]
Simulated	1.42	2.66
Experimental		
1/SSNR	1.27	2.22
1/NRR	1.27	2.17

[a]Experimental efficiency values are evaluated with the mean energy in the ROI.
[b]Experimental errors are evaluated with 1/SSNR or 1/NRR.

For a given criterion, we define the range ratio as the ratio of the maximum to the minimum value of the criterion. Efficiency-range and error-range ratios have comparable respective numerical values in the simulations and the experiments.

6. Conclusion

In this paper, we have proposed a unified approach to the multicriteria design of diffractive optics. The DBS technique has already been proved with respect to its flexibility and its capability to be easily transformed into a multicriteria method, allowing the user to find a trade-off between the diffraction efficiency and the reconstruction accuracy. We have extended this classic multicriteria approach to the IFTA, which helps to dramatically reduce computation times, especially for multilevel domains, without sacrificing the reconstruction accuracy or the diffraction efficiency. So, without increasing the computation time, we have turned the IFTA into an OT technique whose performance can be adapted to the user's requirements and can equal the performance provided by the DBS, whereas the DBS proves to be extremely computer intensive. The experimental reconstructions obtained when binary OT DOEs are displayed on a twisted nematic liquid-crystal SLM confirm the simulations through the evaluation of the efficiency and of a simplified noise criterion.

The authors wish to thank the reviewers for their helpful suggestions, which contributed to making this paper clearer.

References

1. M. A. Seldowitz, J. P. Allebach, and D. W. Sweeney, "Synthesis of digital holograms by direct binary search," Appl. Opt. **26,** 2788–2798 (1987).
2. D. C. Youla, "Image restoration by the method of alternating projections," IEEE Trans. Circuits Syst. **CAS-25,** 694–702 (1978).
3. R. W. Gerchberg and W. O. Saxton, "A practical algorithm for the determination of phase from image and diffraction plane pictures," Optik **35,** 237–246 (1972).
4. F. Wyrowski and O. Bryngdahl, "Iterative Fourier-transform algorithm applied to computer holography," J. Opt. Soc. Am. A **5,** 1058–1065 (1988).
5. L. Legeard, P. Réfrégier, and P. Ambs, "Multicriteria optimality for iterative encoding of computer-generated holograms," Appl. Opt. **36,** 7444–7449 (1997).
6. P. Réfrégier, "Filter design for optical pattern recognition:

multicriteria optimization approach," Opt. Lett. **15,** 854–856 (1990).
7. F. Wyrowski, "Diffraction efficiency of analog and quantized digital amplitude holograms: analysis and manipulation," J. Opt. Soc. Am. A **7,** 383–393 (1990).
8. F. Wyrowski, "Diffractive optical elements: iterative calculation of quantized, blazed phase structures," J. Opt. Soc. Am. A **7,** 961–969 (1990).
9. H. Stark and M. I. Sezan, "Image processing using projection methods," in *Real-Time Optical Information Processing*, B. Javidi and J. L. Horner, eds. (Academic, San Diego, Calif., 1994), pp. 185–232.
10. J. P. Allebach and D. W. Sweeney, "Iterative approaches to computer generated holography," in *Computer Generated Holography II*, S. H. Lee, ed., Proc. SPIE **884,** 2–9 (1988).
11. F. Fetthauer, C. Stroot, and O. Bryngdahl, "On the quantization of holograms with the iterative Fourier transform algorithm," Opt. Commun. **136,** 7–10 (1997).
12. K.-H. Brenner, "Method for designing arbitrary two-dimensional continuous phase elements," Opt. Lett. **25,** 31–33 (2000).
13. L. Legeard, "Étude et optimisation d'hologrammes synthétisés par ordinateur: application au stockage d'informations et aux éléments diffractifs," Ph.D. dissertation (Université de Haute Alsace, Alsace, France, 1995).
14. R. Bräuer, F. Wyrowski, and O. Bryngdahl, "Diffusers in digital holography," J. Opt. Soc. Am. A **8,** 572–578 (1991).
15. J. R. Fienup, "Phase retrieval algorithms: a comparison," Appl. Opt. **21,** 2758–2769 (1982).
16. P. Ambs, L. Bigué, and C. Stolz, "Dynamic computer generated hologram displayed on a spatial light modulator for information processing," in *Euro American Workshop on Optoelectronic Information Processing*, P. Réfrégier and B. Javidi, eds., Vol. CR74 of SPIE Critical Review Series (SPIE Press, Bellingham, Wash., 1999), pp. 151–170.
17. I. Moreno, C. Gorecki, J. Campos, and M. J. Yzuel, "Comparison of computer-generated holograms produced by laser printers and lithography: application to pattern recognition," Opt. Eng. **31,** 3520–3525 (1995).